IEEE Access
Multidisciplinary ⋮ Rapid Review ⋮ Open Access Journal

Received December 13, 2019, accepted January 4, 2020, date of publication January 15, 2020, date of current version January 30, 2020.

Digital Object Identifier 10.1109/ACCESS.2020.2966802

Novel Generalized Predictive Control for Photoelectric Tracking System Based on Improved Objective Function and Predictive Value Correction

JUNHAI QU[1,2], YUANQING XIA[1], (Senior Member, IEEE), SHENGHUI XUE[2], HAIWEN WANG[3], AND YUEDONG MA[2]

[1]School of Automation, Beijing Institute of Technology, Beijing 100081, China
[2]North Automatic Control Technology Institute, Taiyuan 030006, China
[3]School of Electronic Information Engineering, Taiyuan University of Science and Technology, Taiyuan 030024, China

Corresponding author: Junhai Qu (3120160405@bit.edu.cn)

This work was supported in part by the National Natural Science Foundation of China under Grant 61720106010, in part by the Foundation for Innovative Research Groups of the National Natural Science Foundation of China under Grant 61621063, and in part by the Beijing Natural Science Foundation under Grant 4161001.

ABSTRACT Novel generalized predictive control (GPC) is proposed to deal with the problems of cumulative deviation of the predicted value, long control process and large noise that often encountered in conventional GPC. First, the objective function of GPC is improved based on integral time square error (ITSE) criterion, and the output expression under soft constraint is deduced. Then, the predicted value is corrected by adopting the integral weighting method, the convergence of which is demonstrated. Finally, both the simulations and hardware experiments are conducted in a practical photoelectric tracking system. It turns out that the superiority of the improved GPC in control precision, dynamic response and robustness is verified.

INDEX TERMS Generalized predictive control (GPC), integral time square error (ITSE) criterion, objective function, photoelectric tracking system, prediction correction.

I. INTRODUCTION

As a promising control strategy, generalized predictive control (GPC) has drawn much attentions of the researchers in the field, apart from adaptive fuzzy PID, robust control and so on [1]–[5]. By adopting GPC, predictive algorithms are utilized to minimize the cost function and pursue a near-optimal performance of the control system, when taking the system constraints into consideration. Meanwhile, on-line adjustment of important parameters can also be achieved through GPC, which improves the control effect to a large extent [6]–[8]. Therefore, GPC has been widely used in industrial processes, such as metallurgical processes [8], behaviors of the industrial process [9], material transportation [10], temperature control systems [11], [12], and liquid level control systems [13], [14], and so on. Moreover, recent technological advances in the performance and execution speed of microprocessors enables the utilization of GPC in faster processes, such as power systems [15]–[17], aircraft control [18], motor control systems [19]–[22], and overhead cranes with motion-related mechanisms [23].

The effect of GPC is mainly affected by the accuracy of the predictive model, the design of the objective function, and the optimization method. In the past few decades, many studies have been conducted to improve the performance of GPC. For example, an accurate prediction model for the GPC was proposed in [8], along with a neuron adaptive splitting and merging strategy and a weighted parameters adaptive correction approach. Then, another GPC strategy with a closed-loop model identification for burn-through point (BTP) control in the sintering process was presented in [9]. Meanwhile, a feedback linearization GPC strategy was put forward, in which the reference tracking task, the rejection of disturbances, as well as the physical and security constraints were considered [25]. Moreover, a linear GPC for grid-connected voltage-source inverters in a distributed power generation system was also presented, where the parameter λ of the cost function and its effect on bandwidth and robustness was analysis [25].

The associate editor coordinating the review of this manuscript and approving it for publication was Fabio Massaro.

To reduce the performance degradation in the control of signal increments constraints, an event-based GPC control solution with actuator dead band was proposed, and the dead band is modeled as system input constraints in the GPC's optimization procedure [27].

However, when it comes to the control of inertial stabilization platform within photoelectric tracking system, the existing GPC strategies always encounter some problems, such as cumulative deviation of the predicted value, long control process and large noise. Especially in the photoelectric tracking system of unmanned aerial vehicles (UAV), the limited control performance and stabilization accuracy of conventional GPC lead to the shaking of the detected images along with the vehicle's jolting and swaying, which seriously affects the detecting and tracking performance of UAV. To deal with the issue, the prediction error at the current time was used to correct the subsequent predictions [28]. In another attempt, the prediction error at the current time was assigned different weights to correct the subsequent predictions [29]. However, both of the two methods suffer serious cumulative error at any step, and therefore lack robustness.

In this paper, novel GPC based on improved objective function and predictive value correction is proposed. First, the objective function of GPC is improved based on ITSE criterion, and the output expression under soft constraint is deduced. Then, the predicted value is corrected by adopting the integral weighting method, the convergence of which is demonstrated. Finally, both the simulations and hardware experiments are conducted in a practical photoelectric tracking system, to verify the superiority of the improved GPC in control precision, fast dynamic response and robustness.

The remainder of this paper is organized as follows: the improvement of the objective function is introduced in Section II. In Section III, the correction of predicted values is introduced. In addition, the simulation and experiment analysis are conducted, to verify the control effect and robustness of the improved algorithm, as shown in Section IV. Finally, conclusions are presented in Section V.

II. IMPROVEMENT OF OBJECTIVE FUNCTION

The controlled auto-regressive integral moving-average (CARIMA) model is used in GPC to predict the future response of the system. The matrix form of the predictive model is:

$$\hat{Y} = Y^t + G\Delta U + \Xi \tag{1}$$

where Ξ is the effect of noise interference on the output, i.e., an incoherent stationary random sequence with zero means and identical bounded variance.

The future trajectory of the set-point of the system is planned as follows:

$$\begin{cases} w(t-1) = y(t-1|t) \\ w(t+j) = \alpha w(t+j-1) + (1-\alpha)SP(t), \\ \qquad\qquad j = 0, 1, \cdots, p-1 \end{cases} \tag{2}$$

where $SP(t)$ is the set-point of the system at time t, $w(t+j)$ is the softening set-point of the system at time $t+j$, α is the softening factor, and $0 \le \alpha < 1$.

By assuming $W = [w(t),\ w(t+1),\ \ldots,\ w(t+p-1)]^T$, the objective function can be given as:

$$\begin{aligned} &\min_{\Delta U} Z \\ &= \min_{\Delta U} \sum_{j=0}^{p-1} \left\{ [E\left\{\hat{y}(t+j) - w(t+j)\right\}]^2 + \lambda[\Delta u(t-k+j)]^2 \right\} \\ &= \min_{\Delta U} \left[E\left\{(\hat{Y}-W)^T\right\} E\left\{\hat{Y}-W\right\} + \lambda \Delta U^T \Delta U \right] \end{aligned} \tag{3}$$

where λ is the weight of the change of the control quantity.

By default, all predicted control errors have no weight in the objective function. In another words, the errors at any time have the same variation range in the entire control time domain. Generally, however, large error is allowed only at the beginning of the control or when the set-point changes. And the controlled quantity will change with an error within 5%, 2% or less (a large value is not desirable), when converging to the set-point gradually. Therefore, the control error of each step has different variation range.

In this paper, the objective function is improved on the basis of ITSE criterion. Suppose the weight of the prediction error of the j-th step $q_j = f(j)$, and $0 < f(j-1) < f(j)$, obviously, $f(j)$ is an increasing function with respect to j. Q is the positive definite diagonal matrix with q_j as the diagonal element. Hence, the improved objective function can be derived as:

$$\begin{aligned} &\min_{\Delta U} Z \\ &= \min_{\Delta U} \sum_{j=0}^{p-1} \left\{ q_j [E\left\{\hat{y}(t+j) - w(t+j)\right\}]^2 + \lambda[\Delta u(t-k+j)]^2 \right\} \\ &= \min_{\Delta U} \left[E\left\{(\hat{Y}-W)^T\right\} Q E\left\{\hat{Y}-W\right\} + \lambda \Delta U^T \Delta U \right] \\ &\quad s.t. \begin{cases} B_u \le A_U U \le B_U \\ B_u \le [A_U\ A_{\Delta U}] \begin{bmatrix} U \\ \Delta U \end{bmatrix} \le B_U \end{cases} \end{aligned} \tag{4}$$

Constraints are used to limit the control quantity as well as the parameters introduced in Section IV. In this paper, only the soft constraints are considered to limit the output of the control variable. Combining (1) with (4), after taking the expectation, the following can be obtained:

$$\begin{aligned} Z = \left[E\left\{(Y^t + G\Delta U - W)^T\right\} + E\left\{\Xi^T\right\} \right] Q \left[E\left\{Y^t + G\Delta U \right.\right. \\ \left.\left. - W\right\} + E\left\{\Xi\right\} \right] + \lambda \Delta U^T \Delta U \end{aligned} \tag{5}$$

Given that Ξ is random, so $E\{\Xi\} = O$, and $E\left\{\Xi^T\right\} = O^T$, where O is a zero vector. Therefore, the following can be obtained:

$$Z = (Y^t + G\Delta U - W)^T Q (Y^t + G\Delta U - W) + \lambda \Delta U^T \Delta U \tag{6}$$

After expansion, (6) can be rewritten as:

$$Z = (Y^t - W)^T Q (Y^t - W) + \Delta U^T G^T Q (Y^t - W)$$

$$+(Y^t-W)^T QG\Delta U+\Delta U^T G^T QG\Delta U+\lambda\Delta U^T\Delta U \quad (7)$$

Taking the partial derivative with respect to ΔU, we can get

$$\frac{\partial Z}{\partial \Delta U} = G^T Q(Y^t - W) + G^T Q^T (Y^t - W) + G^T QG\Delta U + G^T Q^T G\Delta U + 2\lambda\Delta U \quad (8)$$

Since $Q^T = Q$, the following is obtained:

$$\begin{aligned}\frac{\partial Z}{\partial \Delta U} &= 2G^T Q(Y^t - W) + 2G^T QG\Delta U + 2\lambda\Delta U \\ &= 2G^T Q(Y^t - W) + 2(G^T QG + \lambda I)\Delta U \end{aligned} \quad (9)$$

When $\partial Z/\partial\Delta U = 0$, we can get the improved control increment expression, which can be expressed as:

$$\Delta U = (G^T QG + \lambda I)^{-1} G^T Q(W - Y^t) \quad (10)$$

Note that ΔU cannot exceed its lower and upper limit which are both determined by (4). In another words, when ΔU is less than its lower limit or greater than its upper limit, it will be taken as the lower limit or upper limit.

III. CORRECTION OF PREDICTED VALUES

Prediction error occurs at any prediction step, on account of the modeling errors and interference. As a result, cumulative errors of subsequent predictions emerge because of the rolling effect, given that the control of each step is based on the previous prediction, and the next prediction is based on the current and previous control. Hence, to correct the subsequent prediction, it is crucial to obtain the prediction error, i.e., the deviation of the corresponding prediction.

In this study, the integrals of all the current and previous prediction errors (i.e., the cumulative prediction error) are assigned with different weights to correct the subsequent prediction values.

Theorem 1: Each element of the vector $\hat{Y}$ of predicted values in GPC prediction model increases monotonically with the corresponding element of the known information vector Y^t.

Proof: When (10) is substituted into GPC prediction model, and the effect of noise interference on the output is neglected, the following can be obtained:

$$\hat{Y} = W - [I - G(G^T QG + \lambda I)^{-1} G^T Q](W - Y^t) \quad (11)$$

Given that

$$(G^T QG + \lambda I)^{-1}(G^T QG + \lambda I) = I = (G^T QG + \lambda I)(G^T QG + \lambda I)^{-1} \quad (12)$$

We can get

$$(G^T QG + \lambda I)^{-1} G^T QG = G^T QG(G^T QG + \lambda I)^{-1} \quad (13)$$

Since G is a lower triangular matrix, and the diagonal element is the first term of the unit step response, G is reversible. So the following can be deduced:

$$\begin{aligned}(G^T QG + \lambda I)^{-1} G^T Q &= G^T QG[G(G^T QG + \lambda I)]^{-1} \\ &= G^T QG[(GG^T Q + \lambda I)G]^{-1} \\ &= G^T Q(GG^T Q + \lambda I)^{-1} \end{aligned} \quad (14)$$

Therefore,

$$\begin{aligned} I - G(G^T QG + \lambda I)^{-1} G^T Q &= I - GG^T Q(GG^T Q + \lambda I)^{-1} \\ &= (\frac{1}{\lambda} GG^T Q + I)^{-1} \end{aligned} \quad (15)$$

Given that $GG^T Q/\lambda$ is positive definite, $(GG^T Q/\lambda + I)^{-1}$ is also positive definite. Likewise, $I - G(G^T QG + \lambda I)^{-1} G^T Q$ is also positive definite. From (11), we can find the elements of $\hat{Y}$ increase monotonically with the corresponding elements of Y^t. Therefore, Theorem 1 is proved.

Theorem 2: Prediction error at any time t is $e(t) = y(t) - \hat{y}(t)$. The integral of the prediction error at time t and before is $E(t) = \sum_{i=0}^{t} e(i)$. Note that E is the vector of the weighted integral of prediction errors, and defined as $E = [\varepsilon_1, \varepsilon_2, \cdots, \varepsilon_j, \cdots, \varepsilon_p]^T E(t)$, where $\varepsilon_j = \varepsilon(j) > \varepsilon(j-1) > 0$. Obviously, E is an increasing function with respect to j. Thus, comparing with $\hat{Y}$, the predicted value $\hat{Y}' = \hat{Y} + E$ is closer to the real value Y.

Proof: The predicted output of the future j-th step at time $t+1$ is:

$$\begin{aligned}&\hat{y}'(t+1+j) \\ &\quad = F_j(q^{-1})y(t+1) + G_j(q^{-1})\Delta u(t-k+1+j) + \varepsilon_j E(t).\end{aligned} \quad (16)$$

$\hat{Y}'$ can be described as:

$$\hat{Y}' = Y^{t'} + G\Delta U \quad (17)$$

where $Y^{t'} = Y^t + E$. Suppose "$\prec$" and "$\succ$" are "less than" and "greater than" symbol, respectively. From Theorem 1, if $\hat{Y}(t) \prec Y(t)$,

$$E(t) > 0 \Rightarrow y'(t+1\,|t) > y(t+1\,|t) \Rightarrow \hat{y}'(t+1) > \hat{y}(t+1) \quad (18)$$

which makes the predicted value closer to $y(t+1)$.

If $\hat{Y}(t) \succ Y(t)$,

$$E(t) < 0 \Rightarrow y'(t+1\,|t) < y(t+1\,|t) \Rightarrow \hat{y}'(t+1) < \hat{y}(t+1) \quad (19)$$

which makes the predicted value closer to $y(t+1)$.

If $\hat{Y}(t) = Y(t)$,

$$E(t) = 0 \Rightarrow y'(t+1\,|t) = y(t+1\,|t) \Rightarrow \hat{y}'(t+1) = \hat{y}(t+1) \quad (20)$$

which makes the predicted value equal to $y(t+1)$. At this moment, the control system reaches a steady state. Thus, Theorem 2 is proved.

According to Theorem 2, the prediction error will be significantly reduced, and the prediction accuracy will be obviously improved, after the predicted value is corrected by the integral of the prediction errors. The increment of the control quantity after the correction of prediction is:

$$\Delta U = (G^T QG + \lambda I)^{-1} G^T Q(W - Y^t - E) \quad (21)$$

In practice, the first row is only necessary to be taken as the increment of the control quantity.

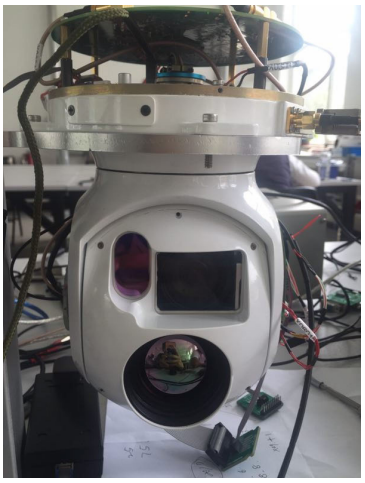

FIGURE 1. The photoelectric tracking system located in an UAV.

IV. APPLICATION

In this study, a 60 V direct current torque motor is used as the actuator for the inertially stabilized platform of the photoelectric tracking system, as shown in Fig. 1. The hardware design of the control board adopts DSP+FPGA architecture. The control quantity is calculated in DSP28335, and then output to FPGA in digital coding form. Then the FPGA calculates the code value and carries out pulse width modulation (PWM) using triangle wave. Finally, motor is controlled by the PWM wave with certain duty ratio.

The block diagram of the load transfer function of the direct current torque motor is shown in Fig. 2. Apparently, no current feedback appears in the control loop. The values of the parameters in Fig. 2 are shown in Table 1.

The transfer function of the motor on-load is:

$$G(s) = \frac{N(s)}{U(s)} = \frac{K_{PC}K_T/R_aJ_Ls(T_es+1)}{1+K_EK_T/R_aJ_Ls(T_es+1)} = \frac{K_{PC}/K_E}{T_mT_es^2+T_ms+1} \tag{22}$$

where $T_m = R_aJ_L/K_EK_T$.

When the unit of the output rate is converted to degrees per second (°/s), the load-transfer function of the motor can be given as:

$$G(s) = \frac{180}{\pi}\frac{K_{PC}/K_E}{T_mT_es^2+T_ms+1} = \frac{0.05358}{0.001667s^2+0.7588s+1} \tag{23}$$

Note that the sampling period of the rate loop is 1 ms. After the discretization through the bilinear method, the discrete transfer function can be deduced as:

$$G(z) = 10^{-6}\frac{6.545+13.09z^{-1}+6.545z^{-2}}{1-1.629z^{-1}+0.6292z^{-2}} \tag{24}$$

Assuming $G(s)$ is the real model of the system, empirically, the coefficient of the denominator of the control model is proportional to that of the mechanism model. After taking the modeling errors into consideration, the model used for the output prediction is:

$$\hat{G}(z) = 10^{-6}\frac{6.545+13.09z^{-1}+6.545z^{-2}}{1-1.873z^{-1}+0.7236z^{-2}} \tag{25}$$

TABLE 1. Values of the parameters shown in figure 2.

Symbol	Meaning	Value
K_{PC}	Drive circuit magnification	0.00375 V
R_a	Armature resistance of the motor	7.1 Ω
L_a	Armature inductance of the motor	15.6 mH
T_e	Electrical time constant of the motor (L_a/R_a)	0.002197 s
K_T	Torque coefficient of the motor	3.5 Nm/A
K_E	Back electromotive force coefficient of the motor	4.01 V/rad·s
J_L	Load moment of inertia	1.5 kg·m^2
T_m	The electromechanical time constant of the motor with load	0.7588 s

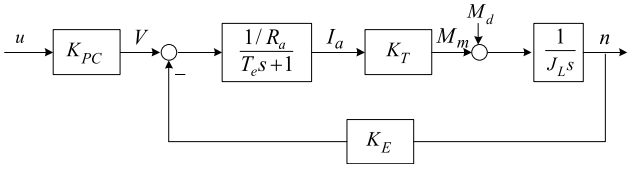

FIGURE 2. Block diagram of the load transfer function of direct current torque motor without current feedback.

A. SIMULATIONS

1) DYNAMIC RESPONSE

An improved generalized predictive controller is designed on the basis of the analyzation shown in Section II and Section III. The parameters of the GPC controller are tuned according to simulation experiments, rather than the selection rules in process control. Actually, the selection rules in process control is not appropriate to the settings of the control parameters, especially α and p, on account of three reasons. Firstly, in process control, α should be set in accordance with the inertia time of the controlled plant to ensure safe operation and timely response of the actuator. Secondly, the determination of p involves the main dynamic part of the step response of the controlled process, and the optimization of dynamic characteristics. Thirdly, the response is always so fast that the sampling period is in milliseconds, but the hardware of the embedded processor cannot meet the requirement of the computing speed. Eventually, through simulation experiments, the parameters of the GPC controller are shown in Table 2.

Comparison of GPC effects with different correction methods of predicted values are shown in Fig. 3. Apart from the correction method appeared in Section III, the correction method proposed in [28] and [29] are also involved. Note that (3) is adopted as the objective function. And the indicators of the control performance of each curve in Fig. 3 are shown in Table 3.

According to Fig. 3 and Table 3, by adopting the proposed correction method, the settling time and the rising time are

TABLE 2. Values of the GPC parameters.

Symbol	Meaning	Value
α	Factor for the reference trajectory	0.73
p	Predictive horizon	6
λ	Weighting factor for increment of the control input	0.000002
A_U	Constraint coefficient matrix for the control input	$0.00375I_{6\times6}$
$A_{\Delta U}$	Constraint coefficient matrix for increment of the control input	$0.00375I_{6\times6}$
B_u	Constraint matrix of the control voltage (lower limit)	$-45\ I_{6\times1}$
B_U	Constraint matrix of the control voltage (upper limit)	$45\ I_{6\times1}$

TABLE 3. Indicators of control performance of GPC effects with different correction methods of predicted values.

Correction Method	q(j)	ε(j)	Rising Time (ms)	Over shoot (%)	Settling Time (ms)
This paper	1	1+1.7(j-1)	26	0	32
Ref. [29]	1	1+1.7(j-1)	28	0	37
Ref. [28]	1	1	30	0	41

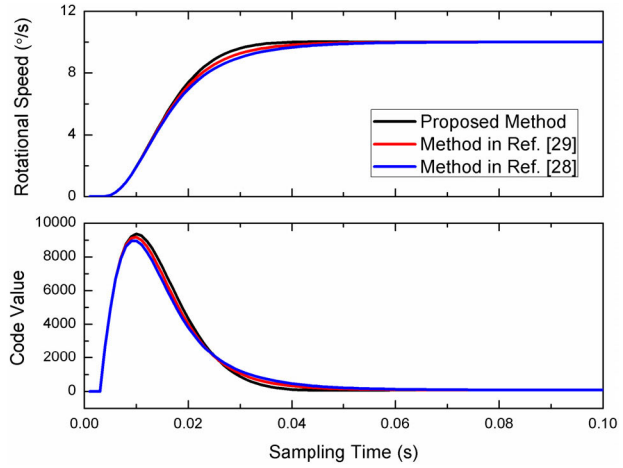

FIGURE 3. Comparison of GPC effects with different correction methods of predicted values.

32 ms and 26 ms, respectively, significantly superior to that by adopting the correction method presented in [28] and [29].

Comparison of GPC effects when the weight $q(j)$ of the prediction error and the weight $\varepsilon(j)$ of the corrected predicted value of the j-th step in the objective function are taking different values are shown in Fig. 4. Note that (4) is adopted as the objective function. And the indicators of the control performance of each curve in Fig. 4 are shown in Table 4.

Comparing with conventional GPC (with $q(j) = 1$, and $\varepsilon(j) = 0$), the best settling time and the rising time by adopting the proposed correction method (with $q(j) = 1+0.1j$, and $\varepsilon(j) = 1+3.4(j-1)$) are 29 ms and 24 ms, respectively, as shown in Fig. 4 and Table 4. Apparently, the response speed of the system is obviously accelerated, after the correction of predicted values using the integral of the prediction error. In another words, a rapid and stabilized control of the system without overshoot is accomplished.

TABLE 4. INdicators of control performance of GPC effects with q(j) and $\varepsilon(j)$ taken different values.

q(j)	ε(j)	Rising Time (ms)	Overshoot (%)	Settling Time (ms)
$1+0.1j$	$1+3.4(j-1)$	24	0	29
1	$1+3.4(j-1)$	23	4.2	41
1	$1+1.7(j-1)$	26	0	32
1	0	31	0	42

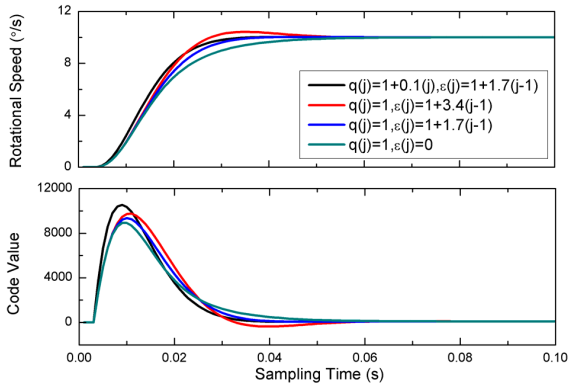

FIGURE 4. Comparison of GPC effects when q(j) and ε(j) are taking different values.

Note that, when $\varepsilon(j)$ is large enough, overshoot will probably appear, leading to the degradation of stability. However, by weighting the control errors in the objective function, the initial response speed of the system will be accelerated. As a result, the stability of the system will eventually be improved.

From (18), the improved design of the objective function can be regarded as the tune of control parameters, similarly, the correction of the predicted values can be regarded as the tuning of control error. Hence, rapid and stabilized control of the photoelectric tracking system is achieved. In another words, the impact of the modeling error is greatly reduced, and the parameters will be matched in short time.

2) STABILITY ACCURACY

When the input of the model is 0°/s, the rocking test with the sinusoidal position disturbance signal with an amplitude of 2° and frequency of 1 Hz is performed. Hence, the effect of stabilized control is shown in Fig. 5.

The stability accuracy can be obtained after the half sine integral of the response curve is calculated and then divided by $2\sqrt{2}$. For the three situations shown in Fig. 5, the rate fluctuation are 0.01868 °/s, 0.02781 °/s, and 0.02984 °/s, respectively. Therefore, the stability accuracy is 0.035 mil, 0.052 mil and 0.056 mil, correspondingly. When the amplitude and frequency of the sinusoidal position disturbance is 5° and 1 Hz, respectively, the effect of stabilized control is shown in Fig. 6.

For the three situations shown in Fig. 6, the rate fluctuation are 0.0467 °/s, 0.06953 °/s, and 0.0746 °/s, respectively. Similarly, the stability accuracy is obtained to be 0.088 mil, 0.13 mil and 0.14 mil, correspondingly. When the amplitude and frequency of the sinusoidal position disturbance is 2° and

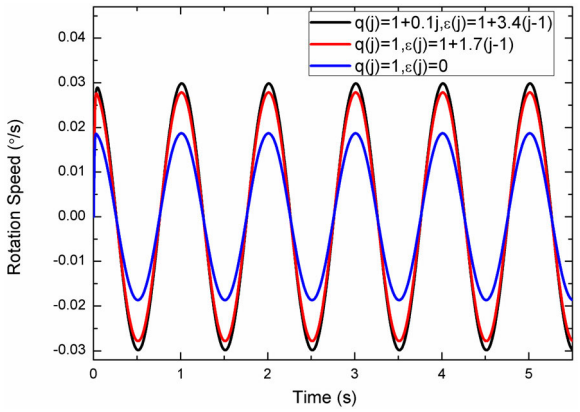

FIGURE 5. Stabilized control effect of GPC when q(j) and ε(j) are taking different values under sinusoidal position disturbance with the amplitude of 2° and the frequency of 1 Hz.

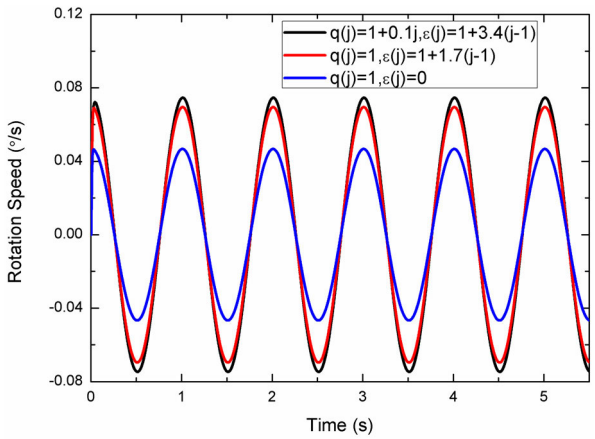

FIGURE 6. Stabilized control effect of GPC when q(j) and ε(j) are taking different values under sinusoidal position disturbance with amplitude of 5° and frequency of 1 Hz.

2 Hz, respectively, the effect of stabilized control is shown in Fig. 7.

For the three situations shown in Fig. 6, the rate fluctuation are 0.1492 °/s, 0.222 °/s, and 0.2374 °/s, respectively. Accordingly, the stability accuracy is 0.14 mil, 0.208 mil and 0.223 mil, correspondingly.

Obviously, the stability accuracy can be significantly improved, by adopting the proposed generalized predictive controller, when sinusoidal position disturbance appears with different amplitudes and frequencies, as shown in Fig. 5, Fig. 6 and Fig. 7.

3) ROBUSTNESS

To investigate the robustness of the proposed GPC, by maintaining the predictive model and control parameters invariant, the control effect of the proposed GPC with different load inertia are shown in Fig. 8. The indicators of the control performance of the curves in Fig. 8 are shown in Table 5.

Apparently, no matter how the load inertia of the plant varies, control effect remains dramatically, which implies the robustness of the proposed GPC. Moreover, due to the soft constraints, the output of the control quantity will not exceed the constraint range.

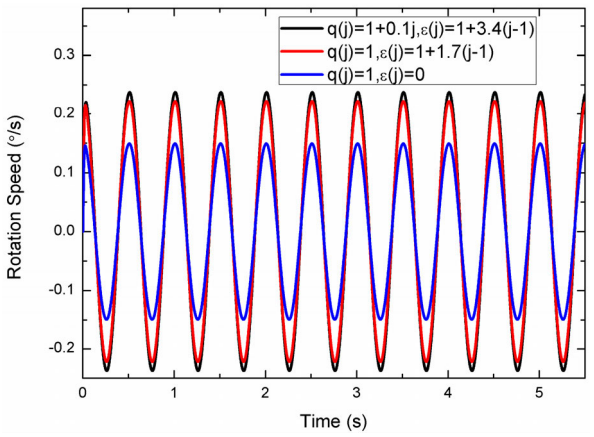

FIGURE 7. Stabilized control effect of GPC when q(j) and ε(j) are taking different values under sinusoidal position disturbance with amplitude of 2° and frequency of 2 Hz.

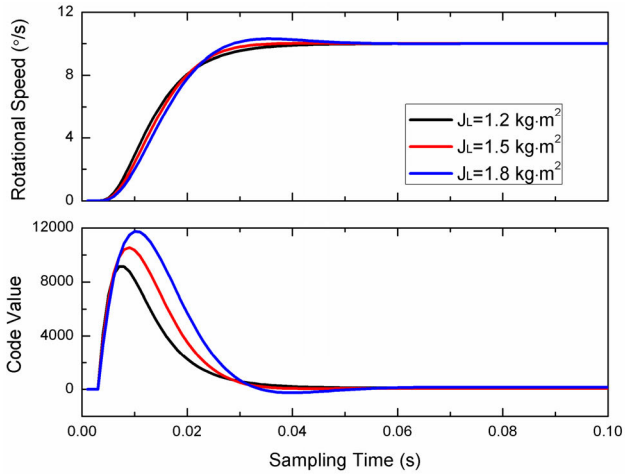

FIGURE 8. Comparison of GPC effects when load inertia is taking different values.

TABLE 5. Indicators of control performance of GPC effects with load inertia taken different values.

Load Inertia J_L (kg·m^2)	q(j)	ε(j)	Rising Time (ms)	Overshoot (%)	Settling Time (ms)
1.2	$1+0.1j$	$1+3.4(j-1)$	25	0	33
1.5	$1+0.1j$	$1+3.4(j-1)$	24	0	29
1.8	$1+0.1j$	$1+3.4(j-1)$	24	3.1	37

B. EXPERIMENTS

Eventually, proposed GPC was applied to the practical photoelectric stabilized servo system. The parameters of α, p, and γ remain invariant, while $q(j)$ and $\varepsilon(j)$ are taking different values. When a square wave signal with an amplitude of 5°/s, period of 4s, and duty ratio of 50% serves as input, the control effect is shown in Fig. 9.

From Fig. 9a, due to the modeling errors, abundant noise is generated in the system and the response rate is rather slow. After the correction of predicted values, the noise in Fig. 9b and 9c is significantly reduced. Meanwhile, the response rate

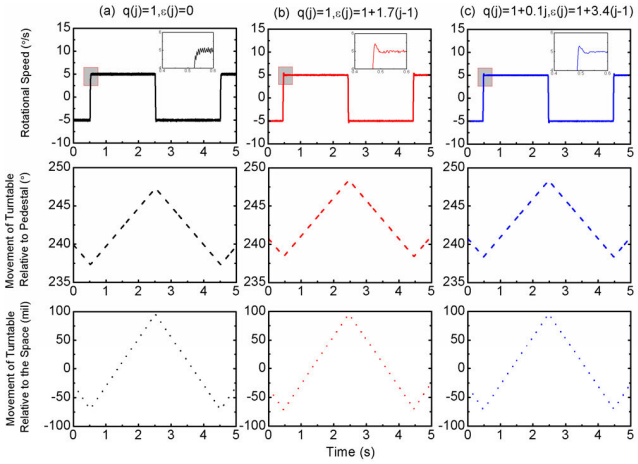

FIGURE 9. Square wave response of GPC to inertially stabilized platform when q(j) and ε(j) are taking different values (a) Square wave response when q(j) = 1 and ε(j)=0, (b) Square wave response when q(j) = 1 and ε(j)=1+1.7(j−1), (c) Square wave response when q(j) =1+0.1j and ε(j) = 1+3.4(j−1).

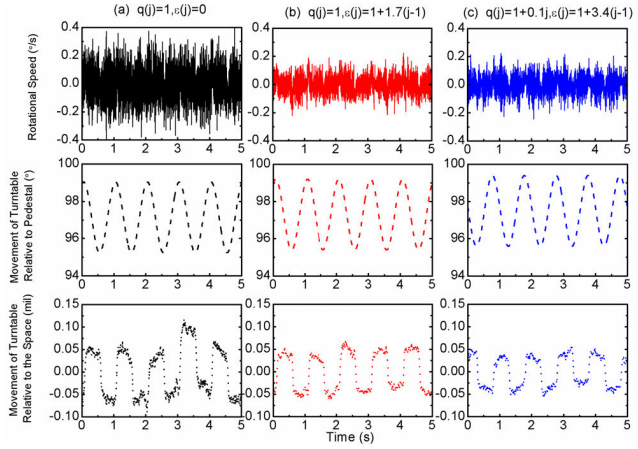

FIGURE 10. Stability control effect of GPC to inertially stabilized platform when q(j) and ε(j) are taking different values (a) Stability control effect when q(j) = 1 and ε(j)=0, (b) Stability control effect when q(j) = 1 and ε(j)=1+1.7(j−1), (c) Stability control effect when q(j) = 1+0.1j and ε(j) = 1+3.4(j−1).

is obviously increased, and an overshoot is generated. After the objective function is improved by weighting, the overshoot in Fig. 9c is dramatically reduced compared to that in Fig. 9b. Therefore, by adopting proposed GPC, rapid and stabilized control of the photoelectric stabilized system is accomplished.

The effect of stability control is shown in Fig. 10, where the turntable input is 0°/s, and the rocking test is also performed. The amplitude and frequency of the sinusoidal position disturbance signal are 2° and 1 Hz, respectively. There is no temporal correspondence between the different pictures, because during the test, not only the positions of the turntable but also the data acquisition period is different. However, the rate curve is temporally correspondence to the position changing curve in the same graph.

The standard deviation of the relative position change of the turntable can be calculated by using least squares method.

TABLE 6. Indicators of stable control of GPC effects with $q(j)$ and $\varepsilon(j)$ taken different values.

q(j)	ε(j)	Rate Noise (°/s)	Relative Position Change of the Turntable (mil)	Stability Accuracy (mil)
$1+0.1j$	$1+3.4(j-1)$	±0.2	±0.06	0.034
1	$1+1.7(j-1)$	±0.2	±0.07	0.049
1	0	±0.4	±0.1	0.054

Simultaneously, the stability accuracy of the turntable can also be obtained. Hence, the indicators of the stabilized control of the curves in Fig. 10 are shown in Table 6.

As illustrated in Fig. 10 and Table 6, the modeling errors leads to a large amount of noise. However, the noise will be significantly decreased, and the stability accuracy will be obviously improved, by adopting the proposed GPC.

V. CONCLUSION

GPC is improved to deal with the problems of cumulative deviation of the predicted value, long control process and large noise. The objective function of GPC is improved based on ITSE criterion, and the output expression under soft constraint is deduced. Meanwhile, the integral weighting method of prediction error is used to correct the predicted value, and the convergence of the method is demonstrated. The superiority of improved GPC in control precision and robustness is verified through the simulation analysis and experimental test in the control of photoelectric tracking system.

However, the proposed GPC increases the number of control parameters. Moreover, the improvement of the objective function and the correction of the predictive value can only be implemented after the control parameters are well tuned through multiple experiments. In the future investigations, improvements of the objective function based on ITAE criterion and the calculation of the control quantity using hard constraints will be conducted.

APPENDIX

NOMENCLATURE

GPC	Generalized Predictive Control
CARIMA	Controlled Auto-Regressive Integral Moving-Average
Ξ	Effect of noise interference on the output
p	Predictive horizon
α	Factor for the reference trajectory
λ	Weighting factor for increment of the control input
Q	Weighting matrix for tracking error
A_U	Constraint coefficient matrix for the control input
$A_{\Delta U}$	Constraint coefficient matrix for increment of the control input
B_u	Constraint matrix of the control voltage (lower limit)
B_U	Constraint matrix of the control voltage (upper limit)

u	Control input (decimal value corresponds to the digital code of the controller output)
K_{PC}	Drive circuit magnification
V	Control voltage
R_a	Armature resistance of the motor
L_a	Armature inductance of the motor
T_e	Electrical time constant of the motor (L_a/R_a)
I_a	Armature current of the motor
K_T	Torque coefficient of the motor
M_m	Output torque of the motor
M_d	Input torque of the disturbance
K_E	Back electromotive force coefficient of the motor
J_L	Load moment of inertia
n	The speed of the rotor (rad/s)
T_m	Electromechanical time constant of the motor with load

REFERENCES

[1] W. Ji, Q. Li, B. Xu, D. Zhao, and S. Fang, "Adaptive fuzzy PID composite control with hysteresis-band switching for line of sight stabilization servo system," *Aerosp. Sci. Technol.*, vol. 15, no. 1, pp. 25–32, Jan. 2011.
[2] J.-P. Song, D. Zhou, G.-L. Sun, and Z.-H. Qi, "Robust control with compensation of adaptive model for dual-stage inertially stabilized platform," *J. Cent. South Univ.*, vol. 25, no. 11, pp. 2615–2625, Dec. 2018, doi: 10.1007/s11771-018-3940-3.
[3] M. Sheikh Sofla, M. Zareinejad, M. Parsa, and H. Sheibani, "Integral based sliding mode stabilizing a camera platform using Kalman filter attitude estimation," *Mechatronics*, vol. 44, pp. 42–51, Jun. 2017, doi: 10.1016/j.mechatronics.2017.04.009.
[4] S. Liu, T. Lu, T. Shang, and Q. Xia, "Dynamic modeling and coupling characteristic analysis of two-axis rate gyro seeker," *Int. J. Aerosp. Eng.*, vol. 2018, Oct. 2018, Art. no. 8513684, doi: 10.1155/2018/8513684.
[5] X. Zhou, B. Zhao, W. Liu, H. Yue, R. Yu, and Y. Zhao, "A compound scheme on parameters identification and adaptive compensation of nonlinear friction disturbance for the aerial inertially stabilized platform," *ISA Trans.*, vol. 67, pp. 293–305, Mar. 2017, doi: 10.1016/j.isatra.2017.01.003.
[6] D. Clarke, C. Mohtadi, and P. Tuffs, "Generalized predictive control—Part I. The basic algorithm," *Automatica*, vol. 23, no. 2, pp. 137–148, Mar. 1987, doi: 10.1016/0005-1098(87)90087-2.
[7] E. F. Camacho and C. Bordons, *Model Predictive Control*, 2nd ed. London, U.K.: Springer-Verlag, 2007.
[8] S. Xie, Y. Xie, T. Huang, W. Gui, and C. Yang, "Generalized predictive control for industrial processes based on neuron adaptive splitting and merging RBF neural network," *IEEE Trans. Ind. Electron.*, vol. 66, no. 2, pp. 1192–1202, Feb. 2019, doi: 10.1109/tie.2018.2835402.
[9] M. Wu, C. Wang, W. Cao, X. Lai, and X. Chen, "Design and application of generalized predictive control strategy with closed-loop identification for burn-through point in sintering process," *Control Eng. Pract.*, vol. 20, no. 10, pp. 1065–1074, Oct. 2012, doi: 10.1016/j.conengprac.2012.05.007.
[10] T. Sato, "Design of a GPC-based PID controller for controlling a weigh feeder," *Control Eng. Pract.*, vol. 18, no. 2, pp. 105–113, Feb. 2010, doi: 10.1016/j.conengprac.2009.12.001.
[11] Y.-L. Chang and C.-C. Tsai, "Adaptive generalised predictive temperature control for air conditioning systems," *IET Control Theory Appl.*, vol. 5, no. 6, pp. 813–822, Apr. 2011, doi: 10.1049/iet-cta.2010.0085.
[12] A. Pawlowski, J. Guzmán, J. Normey-Rico, and M. Berenguel, "Improving feedforward disturbance compensation capabilities in generalized predictive control," *J. Process Control*, vol. 22, no. 3, pp. 527–539, Mar. 2012, doi: 10.1016/j.jprocont.2012.01.010.
[13] Q. Chi, Z. Fei, Z. Zhao, L. Zhao, and J. Liang, "A model predictive control approach with relevant identification in dynamic PLS framework," *Control Eng. Pract.*, vol. 22, pp. 181–193, Jan. 2014, doi: 10.1016/j.conengprac.2013.02.010.
[14] S. Iplikci, "A support vector machine based control application to the experimental three-tank system," *ISA Trans.*, vol. 49, no. 3, pp. 376–386, Jul. 2010, doi: 10.1016/j.isatra.2010.03.013.
[15] M. G. Judewicz, S. A. Gonzalez, N. I. Echeverria, J. R. Fischer, and D. O. Carrica, "Generalized predictive current control (GPCC) for grid-tie three-phase inverters," *IEEE Trans. Ind. Electron.*, vol. 63, no. 7, pp. 4475–4484, Jul. 2016, doi: 10.1109/tie.2015.2508934.
[16] W. Yao, L. Jiang, J. Fang, J. Wen, and S. Wang, "Damping of inter-area low frequency oscillation using an adaptive wide-area damping controller," *J. Elect. Eng. Technol.*, vol. 9, no. 1, pp. 27–36, Jan. 2014.
[17] W. Yao, L. Jiang, J. Wen, Q. Wu, and S. Cheng, "Wide-area damping controller for power system interarea oscillations: A networked predictive control approach," *IEEE Trans. Control Syst. Technol.*, vol. 23, no. 1, pp. 27–36, Jan. 2015, doi: 10.1109/tcst.2014.2311852.
[18] Y. Dai, C. Yang, and C. Wang, "Strategy for robust gust response alleviation of an aircraft model," *Control Eng. Pract.*, vol. 60, pp. 211–217, Mar. 2017, doi: 10.1016/j.conengprac.2016.11.013.
[19] W. Qiao, X. Tang, S. Zheng, Y. Xie, and B. Song, "Adaptive two-degree-of-freedom PI for speed control of permanent magnet synchronous motor based on fractional order GPC," *ISA Trans.*, vol. 64, pp. 303–313, Sep. 2016, doi: 10.1016/j.isatra.2016.06.008.
[20] P. Alkorta, O. Barambones, J. A. Cortajarena, and A. Zubizarrreta, "Efficient multivariable generalized predictive control for sensorless induction motor drives," *IEEE Trans. Ind. Electron.*, vol. 61, no. 9, pp. 5126–5134, Sep. 2014, doi: 10.1109/tie.2013.2281172.
[21] S. Lu, F. Zhou, Y. Ma, and X. Tang, "Predictive IP controller for robust position control of linear servo system," *ISA Trans.*, vol. 63, pp. 211–217, Jul. 2016, doi: 10.1016/j.isatra.2016.02.010.
[22] K. Belda and D. Vosmik, "Explicit generalized predictive control of speed and position of PMSM drives," *IEEE Trans. Ind. Electron.*, vol. 63, no. 6, pp. 3889–3896, Jun. 2016, doi: 10.1109/tie.2016.2515061.
[23] J. Smoczek and J. Szpytko, "Particle swarm optimization-based multivariable generalized predictive control for an overhead crane," *IEEE/ASME Trans. Mechatronics*, vol. 22, no. 1, pp. 258–268, Feb. 2017, doi: 10.1109/tmech.2016.2598606.
[24] M. Beschi, M. Berenguel, A. Visioli, J. L. Guzmán, and L. J. Yebra, "Implementation of feedback linearization GPC control for a solar furnace," *J. Process Control*, vol. 23, no. 10, pp. 1545–1554, Nov. 2013, doi: 10.1016/j.jprocont.2013.02.002.
[25] Y. Kansha and M.-S. Chiu, "Adaptive generalized predictive control based on JITL technique," *J. Process Control*, vol. 19, no. 7, pp. 1067–1072, Jul. 2009, doi: 10.1016/j.jprocont.2009.04.002.
[26] J. Peng, R. Dubay, J. M. Hernandez, and M. Abu-Ayyad, "A wiener neural network-based identification and adaptive generalized predictive control for nonlinear SISO systems," *Ind. Eng. Chem. Res.*, vol. 50, no. 12, pp. 7388–7397, Jun. 2011, doi: 10.1021/ie102203s.
[27] A. Pawlowski, A. Cervin, J. L. Guzman, and M. Berenguel, "Generalized predictive control with actuator deadband for event-based approaches," *IEEE Trans. Ind. Informat.*, vol. 10, no. 1, pp. 523–537, Feb. 2014, doi: 10.1109/tii.2013.2270570.
[28] B. P. Wang, S. Y. Li, and T. Zhou, "Steady-state objective optimization in model predictive control and its application," *Syst. Eng. Electron.*, vol. 31, no. 6, pp. 1429–1431, 2009.
[29] D. Q. Shu and Z. S. Shi, "Global Convergence of Implicit Self-tuning Generalized Predictive Controller," *ACTA Autom. Sin.*, vol. 21, no. 5, pp. 545–554, 1995.

JUNHAI QU was born in Shanxi, China, in 1979. He received the double B.S. degrees in automatic control and computer science and technology from the Taiyuan University of Science and Technology, Taiyuan, China, in 2001, and the M.S. degree in software engineering from the Beijing Institute of Technology, Beijing, China, in 2011, where he is currently pursuing the Ph.D. degree with the School of Automation.

From 2010 to 2018, he was a Senior Engineer with the North Automatic Control Technology Institute, Taiyuan, China. He has published some articles in relevant area and holds five patents. His research interests include gyroscopes filtering algorithms, sensor data processing methods, automatic control technologies, and design of motion control systems.

YUANQING XIA (Senior Member, IEEE) was born in Anhui, China, in 1971. He received the M.S. degree in fundamental mathematics from Anhui University, China, in 1998, and the Ph.D. degree in control theory and control engineering from the Beijing University of Aeronautics and Astronautics, Beijing, China, in 2001. From 2002 to 2003, he was a Postdoctoral Research Associate with the Institute of Systems Science, Academy of Mathematics and System Sciences, Chinese Academy of Sciences, Beijing, where he worked on navigation, guidance and control. From November 2003 to February 2004, he was a Research Fellow with the National University of Singapore, where he worked on variable structure control. From February 2004 to February 2006, he was with the University of Glamorgan, Pontypridd, U.K., as a Research Fellow, where he worked on networked control systems. From February 2007 to June 2008, he was a Guest Professor with Innsbruck Medical University, Innsbruck, Austria, where he worked on biomedical signal processing. Since July 2004, he has been with the School of Automation, Beijing Institute of Technology, Beijing, first as an Associate Professor, then, since 2008, as a Professor.

He is currently the Dean with the School of Automation, Beijing Institute of Technology. His current research interests are in the fields of networked control systems, robust control and signal processing, active disturbance rejection control and flight control.

SHENGHUI XUE was born in Shanxi, China, in 1989. He received the B.S. degree in measurement control technology and instrument from the Kunming University of Science and Technology, Kunming, China, in 2011, and the M.S. degree in control theory and control engineering from the University of Science and Technology of China, Hefei, China, in 2014.

He is currently a Control Engineer in servomechanism with the North Automatic Control Technology Institute, Taiyuan, China. His research interests include the fast and smooth control, disturbance rejection control, and optimal control for gyroscope-stabilized platform. He has published some articles in his research area.

HAIWEN WANG was born in Hebei, China, in 1977. She received the double B.S. degrees in automatic control and computer science and technology from the Taiyuan University of Science and Technology, Taiyuan, China, in 2001, and the M.S. degree in computer science and technology from the Taiyuan University of Science and Technology, Taiyuan, in 2006.

From 2011 to 2018, she was an Associate Professor with the Taiyuan University of Science and Technology. Her research interests include intelligent control, 2-DOF, and the design of servo systems. She has published some articles in relevant area.

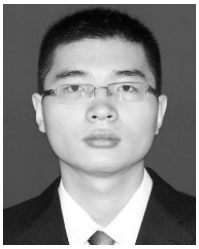

YUEDONG MA was born in Shanxi, China, in 1987. He received the B.S. degree in optical information science and technology from the North University of China, Taiyuan, China, in 2009, and the Ph.D. degree in optical engineering from Chongqing University, Chongqing, China, in 2016.

He is currently an Associate Research Fellow with the North Automatic Control Technology Institute, Taiyuan. His research interests include automatic control technologies, synergetic control, and intelligent decision making for multiagent systems.